


RESEARCH

Open Access



Role of SIK1 in the transition of acute kidney injury into chronic kidney disease

Jinxu Hu^{1†}, Jiao Qiao^{1†}, Qun Yu¹, Bing Liu^{1,2}, Junhui Zhen³, Yue Liu¹, Qiqi Ma², Yanmei Li¹, Qianhui Wang², Cheng Wang² and Zhimei Lv^{1,2*} 

Abstract

Background: Acute kidney injury (AKI), with a high morbidity and mortality, is recognized as a risk factor for chronic kidney disease (CKD). AKI-CKD transition has been regarded as one of the most pressing unmet needs in renal diseases. Recently, studies have showed that salt inducible kinase 1 (SIK1) plays a role in epithelial-mesenchymal transition (EMT) and inflammation, which are the hallmarks of AKI-CKD transition. However, whether SIK1 is involved in AKI-CKD transition and by what mechanism it regulates AKI-CKD transition remains unknown.

Methods: We firstly detected the expression of SIK1 in kidney tissues of AKI patients and AKI mice by immunohistochemistry staining, and then we established Aristolochic acid (AA)-induced AKI-CKD transition model in C57BL/6 mice and HK2 cells. Subsequently, we performed immunohistochemistry staining, ELISA, real-time PCR, Western blot, immunofluorescence staining and Transwell assay to explore the role and underlying mechanism of SIK1 on AKI-CKD transition.

Results: The expression of SIK1 was down-regulated in AKI patients, AKI mice, AA-induced AKI-CKD transition mice, and HK2 cells. Functional analysis revealed that overexpression of SIK1 alleviated AA-induced AKI-CKD transition and HK2 cells injury in vivo and in vitro. Mechanistically, we demonstrated that SIK1 mediated AA-induced AKI-CKD transition by regulating WNT/ β -catenin signaling, the canonical pathway involved in EMT, inflammation and renal fibrosis. In addition, we discovered that inhibition of WNT/ β -catenin pathway and its downstream transcription factor Twist1 ameliorated HK2 cells injury, delaying the progression of AKI-CKD transition.

Conclusions: Our study demonstrated, for the first time, a protective role of SIK1 in AKI-CKD transition by regulating WNT/ β -catenin signaling pathway and its downstream transcription factor Twist1, which will provide novel insights into the prevention and treatment AKI-CKD transition in the future.

Keywords: AA, SIK1, AKI-CKD transition, Wnt/ β -catenin, Twist1

Background

Acute kidney injury (AKI), a common disease characterized by a decrease in glomerular filtration rate (GFR) and an increase in serum creatinine [1], is regarded as a risk factor for the development and progression of CKD

[2, 3]. Recently, AKI-CKD transition has become one of the hotspots in the study of kidney diseases. Although it is reported that inflammation, EMT, and fibrosis play a vital role in the progress of AKI-CKD transition [4, 5], the exact molecular mechanism of AKI-CKD transition is still unclear.

Salt Inducible Kinase 1 (SIK1) is a member of the AMP-activated protein kinases (AMPKs) family, which play pivotal roles in regulating metabolism, cell survival, and growth [6, 7]. Studies have demonstrated that inhibition of SIK1 promotes EMT, leading to migration and

*Correspondence: sdlvzhimei@163.com

[†]Jinxu Hu and Jiao Qiao contributed equally to this work.

²Department of Nephrology, Shandong Provincial Hospital Affiliated to Shandong First Medical University, Jinan 250021, Shandong, China
Full list of author information is available at the end of the article



metastasis of tumors [8–10]. Besides, it was reported that SIK1 negatively regulate the TLR4-induced activation of NF- κ B and attenuated expressions of proinflammatory cytokines [11]. In addition, emerging evidences showed a link between SIK1 and kidney diseases [6, 12]. For instance, upregulation of SIK1 reversed the high glucose-induced mesangial cells proliferation, and extracellular matrix (ECM) accumulation by inhibiting the expression of FN and PAI-1, both of which are involved in fibrotic disorders, such as glomerulosclerosis [6, 13]. Thus, we speculate that SIK1 might be involved in the progression of AKI-CKD transition, which is characterized with EMT, inflammation and renal fibrosis.

WNT/ β -catenin pathway is a complex, highly conserved signaling pathway that regulates various biologic processes, such as organ development, tissue homeostasis and carcinogenesis [14, 15]. Although silent in the normal adult kidney, it is found to be reactivated in a variety of kidney diseases, including acute kidney injury, diabetic nephropathy, interstitial fibrosis and cystic kidney diseases [16]. Moreover, it is reported that silencing of WNT/ β -catenin pathway ameliorates renal fibrosis, delaying the progression of AKI-CKD in I/R-induced injury [17]. But whether SIK1 could participate in the AKI-CKD transition by modulating WNT/ β -catenin pathway remains to be further clarified.

Emerging evidences have shown that Snail and Twist1, the EMT transcription factors, play important roles in the pathogenesis of renal fibrosis [18–20]. It was reported that conditional deletion of Twist1 or Snail in proximal tubular epithelial cells inhibited EMT, attenuated interstitial fibrosis in experimentally induced renal fibrosis in mouse [21]. Considering Snail and Twist1 are significant molecules located in the downstream of WNT/ β -catenin pathway, we speculated that they may also played a vital role in SIK1 mediated AKI-CKD transition.

Thus, in this study, we aimed to elucidate the role and mechanism of SIK1 in AKI-CKD transition, which will provide a new therapeutic target for clinical prevention and treatment of renal fibrosis and will provide a new way to delay the progress of AKI-CKD transition.

Materials and methods

Patients and tissue samples

The study was approved by the Clinical Research Ethics Committee of Shandong Provincial Hospital Affiliated to Shandong University. Human kidney samples were collected from patients with AKI diagnosed based on renal biopsy, and the kidney samples in the control groups were obtained from paracancerous tissue of patients with kidney tumors who underwent surgical resection. The tissue samples were preserved in liquid nitrogen and the

informed consent was signed by all patients in accordance with the Declaration of Helsinki.

Construction of AAV9-*Sik1*

Recombinant adeno-associated virus (AAV9-*Sik1*) and adeno-associated virus negative control (AAV9-NC) were constructed by GENECHM (Shanghai, China). Recombinant AAV9-*Sik1* adeno-associated virus vector GV467 includes promoter, antibody coding region, EGFP green fluorescent protein coding region, and 3FLAG tag protein coding region. The ability of AAV9 vector to transduce kidney has been verified (Additional file 1).

Animals and modeling methods

Modeling and follow-up experimental programs have been approved by the Animal Care and Use Committee of Shandong University. C57BL/6 mice aged 4–6 weeks and weighing 15–20 g were supplied by the Experimental Animal Center of Shandong University and were randomly allocated into 4 groups: control group (Control), normal mice treated with AA group (AA), AA mice treated with AAV9-*Sik1* group (AAV9-*Sik1* + AA), AA mice treated with AAV9-NC group (AAV9-NC + AA). The mice in AA group were injected with AA (10 mg/kg) intraperitoneally, while the mice in control group were injected with PBS. On the 3rd, 7th, 14th, and 28th after AA injection, the 24 h urine of mice was collected in a metabolic cage and the supernatant was stored at -20°C after centrifugation. Blood was centrifuged at 3000r for 10 min, and the supernatant was stored at -20°C . 24 h urinary protein, serum creatinine (Scr), and blood urea nitrogen (BUN) were measured by automatic biochemical analyzer. Serum IL-1 β and TNF- α were detected by ELISA. Then, the mice were sacrificed and weighed. After that kidneys were excised and weighed. All kidney samples were divided into two parts, one of which was fixed in 4% paraformaldehyde for histological staining, while the other was stored under -80°C for real-time PCR and Western blot detection.

Histology and immunohistochemistry

After fixing in 4% paraformaldehyde, the kidney samples were dehydrated, transparent, embedded in paraffin and sectioned into 4 μm -thick slices. Subsequently, the slices were dewaxed, hydrated and stained. For renal histological analysis, HE staining, PAS staining and Masson's trichrome staining were used according to the manufacturer's instructions. For immunohistochemical analysis, sections were incubated with primary antibody against SIK1(51045-1-AP, Proteintech, USA), E-cadherin (20874-1-AP, Proteintech, USA), α -SMA (ab32575, Abcam, USA), COL1 (bs-10423R, Bioss, Beijing, China) at 4°C overnight. After incubation with secondary

antibody, the DAB was added, followed by nuclear counterstaining with hematoxylin. Finally, the images were observed under microscope (Leica, Germany). The percentage of positive staining for SIK1, E-cadherin, α -SMA, and COL1 was measured by using a quantitative Image-Pro plus 6.0 software (Media Cybernetics, Silver Spring, MD) [22].

Cell culture and treatment

Human proximal tubular epithelial cells (HK2) were cultured in DMEM medium (Gibco, USA) supplemented with 10% fetal bovine serum (FBS) (Gibco, USA) and 1% penicillin–streptomycin (Sigma, USA) at 37 °C in a humidified atmosphere containing 5% CO₂. Aristolochic acid (AA) (Sigma, USA) was dissolved in DMSO to 1 mg/mL and cells were treated with the final concentration at 10 μ mol/L, 20 μ mol/L, 40 μ mol/L and 60 μ mol/L, and the control group was treated with the same amount of DMSO.

Lentiviral vector transduction and siRNA transfection

The lentiviral shRNA constructs targeting *SIK1*, β -catenin and a scrambled shRNA, as well as lentiviral overexpression vector for *SIK1* and empty control vector were constructed by Cyagen (Guangzhou, China). The target sequences are listed as follows: *SIK1* shRNA: 5'-GCGCGTGCATTGATTACTATC-3'; β -catenin shRNA: 5'-TTTGATCCCATCTTCCGCAGC-3'; Scrambled shRNA: 5'-CCTAAGGTTAAGTCGCCCTCG-3'. The lentivirus infection was conducted following the standard protocol provided by the manufacturer. *Twist1* siRNA and a negative control sequence (NC siRNA) were designed by RiboBio (Guangzhou, China). The target sequences were listed as follows: *Twist1* siRNA: 5'-CCGGAGACCTAGATGTCAT-3'; NC siRNA: 5'-UUCUCCGAACGUGUCACGUTT-3'. Transfection of HK2 cells was performed in a 6-well plate using LipofectamineTM2000 (Invitrogen, USA) according to the manufacturer's instructions.

Cell counting kit-8 (CCK-8)

Cells were seeded in a 96-well plate at a density of 2×10^4 /mL and then treated with different concentrations of AA (10, 20, 40, 60 μ mol/L) in an incubator containing 5% CO₂ at 37 °C. After 72 h treatment, 10 μ L of CCK-8 solution (YESEN, Shanghai, China) was added into each well. After incubation for 1.5 h, the absorbance at 450 nm of each well was measured with a microplate reader (Thermo Fisher Scientific, USA). Five replicated

wells were used for different groups and experiments were performed in triplicate.

Enzyme-linked immunosorbent assay (ELISA)

The concentrations of IL-1 β and TNF- α in the serum or in the supernatant of treated HK2 cells were collected and detected using ELISA Kit (ColorfulGene, Wuhan, China) according to the manufacturer's instructions. The absorbance O.D. was read at 450 nm using a Microtiter Plate Reader.

RNA extraction and quantitative real-time PCR analysis

Total RNA was extracted from HK2 cells or kidney tissues using TRIzol reagent (Takara, Japan). RNA purity was assessed using a NanoDrop-2000 spectrophotometer (Thermo Fisher Scientific, USA) and each RNA sample had an A260:A280 above 1.8 and A260:A230 above 2.0. Subsequently, 1.0 μ g RNA from each sample were reverse transcribed using the PrimeScriptTM RT Reagent Kit (Takara, Japan) according to the manufacturer's instructions and PCR amplification was performed using SYBR[®] Premix Ex Taq (Takara, Japan) in the LightCycler[®] 480 Real-Time PCR system (Roche, USA). The sequences of primers used in qPCR were listed in Additional table. β -actin was used as the internal control and the relative expression levels were calculated using the $2^{-\Delta\Delta CT}$ method. All the reactions were repeated in triplicate.

Western blot analysis

After cells or kidney tissues were fully lysed with RIPA lysate (Beyotime, China) containing protease inhibitor and phosphorylated protease inhibitor, the protein was denatured. Then about 20 μ g of protein was separated using SDS-PAGE and transferred to PVDF membranes (Millipore, USA). Subsequently, the membranes were blocked in 5% non-fat milk powder or 5% BSA for 1 h at room temperature in order to break non-specific binding, followed by incubation with primary antibody against SIK1 (51045-1-AP, Proteintech, USA), Caspase1/p20/p10 (22915-1-AP, Proteintech, USA), E-cadherin (20874-1-AP, Proteintech, USA), Vimentin (60330-1-Ig, Proteintech, USA), p-SIK1(Thr182)(PA5-105918, Thermo Fisher Scientific, USA), WNT1(ab15251, Abcam, USA), β -catenin(ab32572, Abcam, USA), p- β -catenin(Y654)(ab59430, Abcam, USA), ZO-1(ab96587, Abcam, USA), α -SMA(ab32575, Abcam, USA), Fsp1(ab197896, Abcam, USA), FN(ab2413, Abcam, USA), β -actin(ab8227, Abcam, USA), Histone 3(ab176842, Abcam, USA), COL1 (bs-10423R, Bioss, Beijing, China), Snail(#3879, Cell Signaling Technology, USA), and Twist1(#46702, Cell Signaling Technology, USA) at 4 °C overnight. After incubation with horseradish peroxidase-conjugated goat

anti-rabbit IgG (ab6721, Abcam, USA) or horseradish peroxidase-conjugated goat anti-mouse IgG (ab6728, Abcam, USA) for 1 h at room temperature, the results were analysis using ECL reagent (Millipore, USA) and Amersham Imager 600 (GE, USA). β -actin was used as an internal control of total proteins, and Histone 3 was used as an internal control of nuclear proteins.

Immunofluorescence staining

Cells were plated in 24-well slides followed by different interventions and then fixed with 4% paraformaldehyde. After penetration with 0.3% Triton X-100, the cells were incubated with 5% BSA for 30 min at room temperature. Next, the cells were incubated with β -catenin, E-cadherin, and Vimentin antibody at 4 °C overnight. Subsequently, Alexa Fluor[®] 594-conjugated donkey anti-rabbit IgG (ab150076, 1:200, Abcam, USA) and Alexa Fluor[®] 594-conjugated goat anti-mouse IgG (ab150116, 1:200, Abcam, USA) antibodies were applied for 1 h at 37 °C protected from light. After incubation with DAPI for 10 min, the cells were observed with a fluorescence microscope (Leica, Germany).

Transwell migration assay

For the Transwell assay, $1-2 \times 10^4$ /mL HK2 cells in 150 μ L serum-free medium were added to the upper chamber of Transwell and 600 μ L DMEM medium containing 10% FBS were added to the lower chamber. Next, the cells were incubated at 37 °C for 24 h, and then fixed with 4% paraformaldehyde, and penetrated with 0.3% Triton X-100. After that, the non-invading cells were removed, the invaded cells were dyed with hematoxylin and then counted under a light microscope (Olympus, Japan).

Statistical analysis

GraphPad Prism 8 and Adobe Photoshop were used to analyze experimental data and draw statistical graphs. The results were shown as the mean \pm s.d. Statistical significance between two groups was determined by Student t-test while significance among multiple groups was determined by one-way ANOVA. $P < 0.05$ indicated a statistically significant difference. All experiments were repeated at least three times unless otherwise stated.

Results

SIK1 was down-regulated in AKI

Considering that SIK1 plays a significant role in kidney injury, we firstly detected the expression of SIK1 in kidney tissues of AKI patients and AKI mice. Immunohistochemistry staining revealed that, not only in patients but in mice, the SIK1 expression of renal tubules in control is higher than that in AKI group, which indicated that SIK1

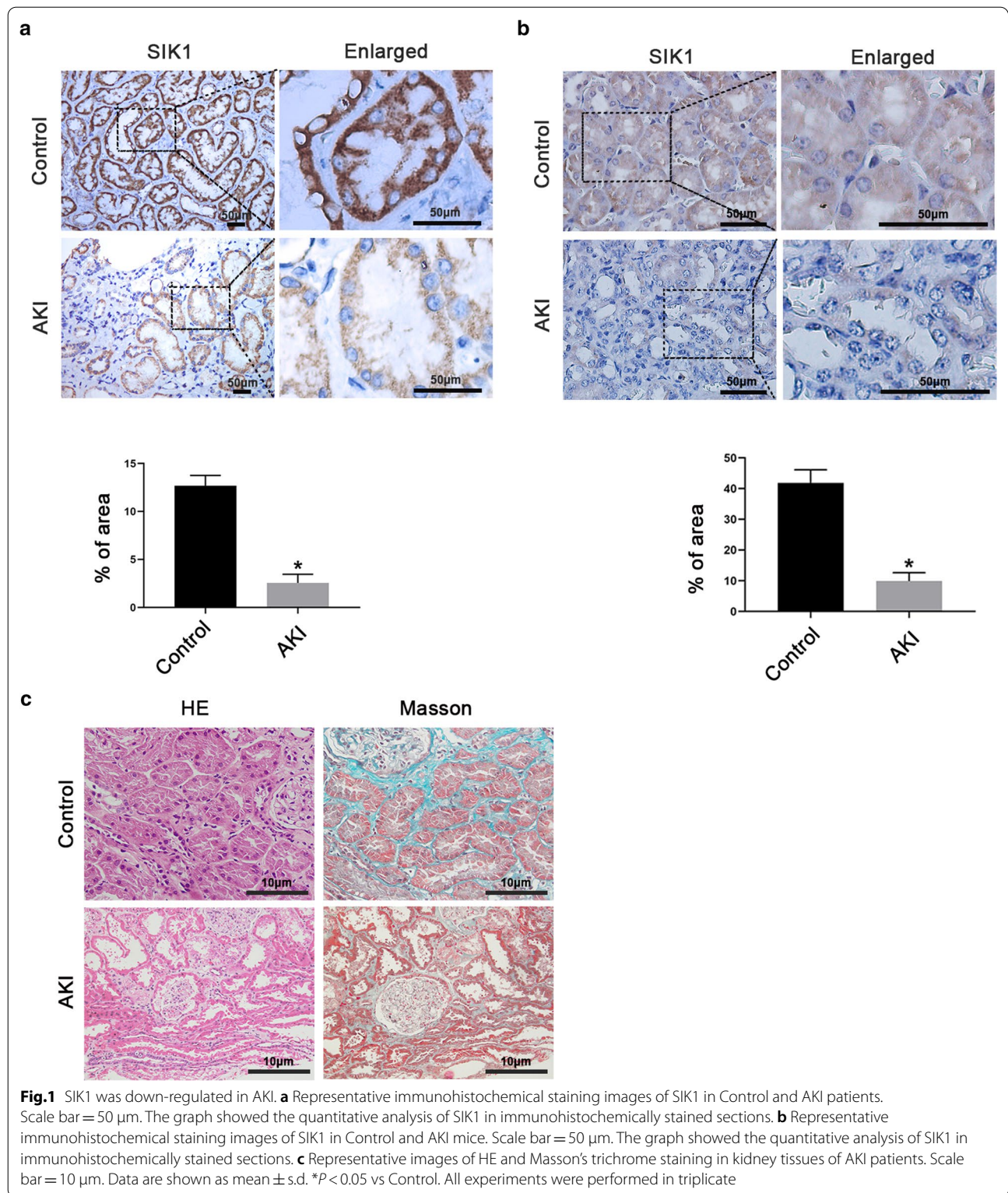
was down-regulated during AKI (Fig. 1a, b). Besides, we conducted HE and Masson's trichrome staining to analyze the histopathological changes in kidney samples of AKI patients (Fig. 1c). Compared with control, renal tubular epithelial cells swelling, vacuolar degeneration, and interstitial edema were observed in the AKI group by HE staining. Moreover, compared with control, notably flattened tubular cells, detached brush border, and enlarged tubular limens were observed in AKI group by Masson's trichrome staining. Taken together, all these findings indicated that SIK1 might play a role in tubular injury.

SIK1 was down-regulated in AA-induced AKI-CKD transition mice

To obtain a mice model of AKI-CKD transition, we injected AA intraperitoneally into mice. Compared with control, the mice treated with AA exhibited increased production of inflammatory factors, EMT and renal fibrosis (Fig. 2a–d). In addition, the kidney index, serum Scr, BUN and 24 h urinary protein enhanced upon AA treatment (Fig. 2e). Furthermore, AA impaired renal structure, leading to renal tubular epithelial cells atrophy, lumen enlargement, and different extent of collagen fiber deposition in tubulointerstitium (Fig. 2f). All above indicated that the AA-induced AKI-CKD transition model was successfully established. To explore the role of SIK1 in AA-induced AKI-CKD transition, we assessed its expression in the samples of mice kidney injected with AA. We found SIK1 and p-SIK1 (Thr182) were decreased in a time-dependent manner after AA injection (Fig. 2g), which indicating a potential role for SIK1 in regulating AA-induced AKI-CKD transition.

Overexpression of SIK1 alleviated AA-induced AKI-CKD transition

To specify the function of SIK1 in AA-induced AKI-CKD transition, we injected AAV9-*Sik1* into tail vein of mice to overexpress SIK1. We found after injected with AAV9-*Sik1*, AA-induced renal dysfunction was significantly ameliorated, as evidenced by reduced levels of kidney index, Scr, BUN and 24 h urinary protein (Fig. 3a). Real-time PCR revealed that AAV9-*Sik1* relieved AA-induced inflammatory response (Fig. 3b). In addition, AAV9-*Sik1* significantly improved the histopathological damage induced by AA (Fig. 3c). Furthermore, the results of immunohistochemical staining suggested that AAV9-*Sik1* alleviated interstitial fibrosis and EMT in the process of AA-induced AKI-CKD transition (Fig. 3d). Overall, these results indicated that SIK1 played a protective role in AA-induced AKI-CKD transition.



SIK1 was down-regulated in AA-treated HK2 cells

A large number of studies have shown that the proximal tubule of the kidney is one of the main targets of injury

in AKI, and the injury of proximal tubule may play an important pathophysiologic role in the development of AKI-CKD transition. To further assess whether SIK1 was

(See figure on next page.)

Fig. 2 SIK1 was down-regulated in AA-induced AKI-CKD transition mice. **a** ELISA analysis of IL-1 β , and TNF- α expression in different groups of mice. **b** Western blot and real-time PCR analysis of inflammation and fibrosis markers (Caspase1/p20/p10, FN and COL1) expression; **c** Western blot and real-time PCR analysis of EMT markers (E-cadherin, Vimentin, and α -SMA) expression. **d** Representative immunohistochemical staining images of E-cadherin in different groups of mice. Scale bar = 50 μ m. The graph showed the quantitative analysis of E-cadherin in immunohistochemically stained sections. **e** The kidney index, Scr, BUN and 24 h urinary protein levels in different groups of mice. **f** Representative histological staining (HE, PAS, and Masson's trichrome staining) images of kidney tissues in different groups of mice. Scale bar = 50 μ m. **g** Western blot analysis of SIK1 and p-SIK (Thr182) protein levels in C57BL/6 mice. Data are shown as mean \pm s.d. * P < 0.05 vs Control. All experiments were performed in triplicate

down-regulated *in vitro*, we focused on HK2 cells in this study. By performing CCK8 assays, we choose 10 μ mol/L AA as the optimal concentration for subsequent experiments (Additional file 2). Consistently, AA treatment exhibited increased inflammation, EMT and fibrosis in HK2 cells (Fig. 4a–c), suggesting AA induced HK2 cells injury *in vitro*. Subsequently, we examined the protein levels of SIK1 and observed a notably decreased SIK1 and p-SIK1 (Thr182) in HK2 cells in the presence of AA (Fig. 4d). Furthermore, we detected the location of SIK1 protein in HK2 cells before and after exposure to AA by Immunofluorescence staining. In the unstimulated cells, SIK1 was observed in both the nucleus and cytoplasm. When treated with AA, the expression of SIK1 was reduced and the SIK1 was gradually detected in the nucleus (Additional file 3). Collectively, these results elucidated that SIK1 was involved in AA-induced HK2 cells injury.

Overexpression of SIK1 improved AA-induced HK2 cells injury

To further elucidate the role of SIK1 in AA-induced HK2 cells injury, we constructed cell lines that stably up-regulated SIK1 by lentivirus infection of HK2 cells (Additional file 4). Overexpression of SIK1 led to a significantly increased E-cadherin and repressed Caspase1/p20/p10, Vimentin, COL1, and Eps1, when compared with the control cells stimulated with AA alone (Fig. 4e, f). Besides, overexpression of SIK1 inhibited the migration ability of HK2 cells induced by AA (Fig. 4g). Together, these findings demonstrated that SIK1 was protective against AA-induced injury in HK2 cells.

SIK1 regulated WNT/ β -catenin signaling pathway *in vivo* and *in vitro*

Considering the critical role of the WNT/ β -catenin pathway in AKI-CKD transition, we explored whether SIK1 regulated WNT/ β -catenin pathway. *In vivo* experiments, we observed that overexpression of SIK1 inhibited the protein levels of WNT1, p- β -catenin (Y654), and nuclear β -catenin in AA-induced AKI-CKD mice (Fig. 5a). To further explore whether SIK1 regulated WNT/ β -catenin pathway *in vitro*, we silenced the expression of SIK1 by shRNA in HK2 cells

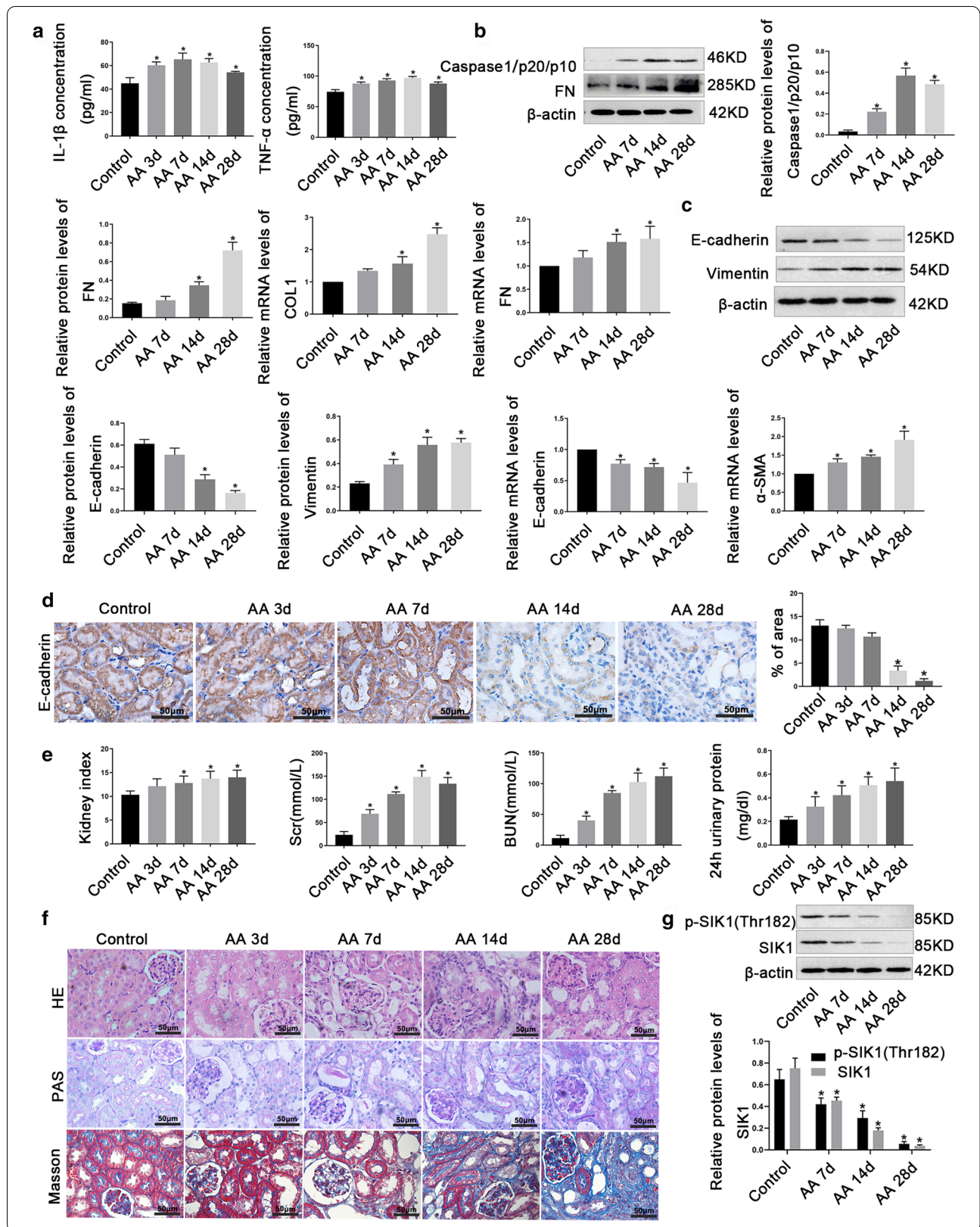
(Additional file 5). Consistent with the *in vivo* results, silencing of SIK1 resulted in a notably increased β -catenin, *TCF4* and *LEF1* mRNA levels (Fig. 5b). Besides, knockdown of SIK1 increased the protein levels of β -catenin and p- β -catenin (Y654) (Fig. 5c). In addition, knockdown of SIK1 promoted the nuclear translocation of β -catenin (Fig. 5d). Collectively, these data suggested that SIK1 regulated WNT/ β -catenin pathway *in vivo* and *in vitro*.

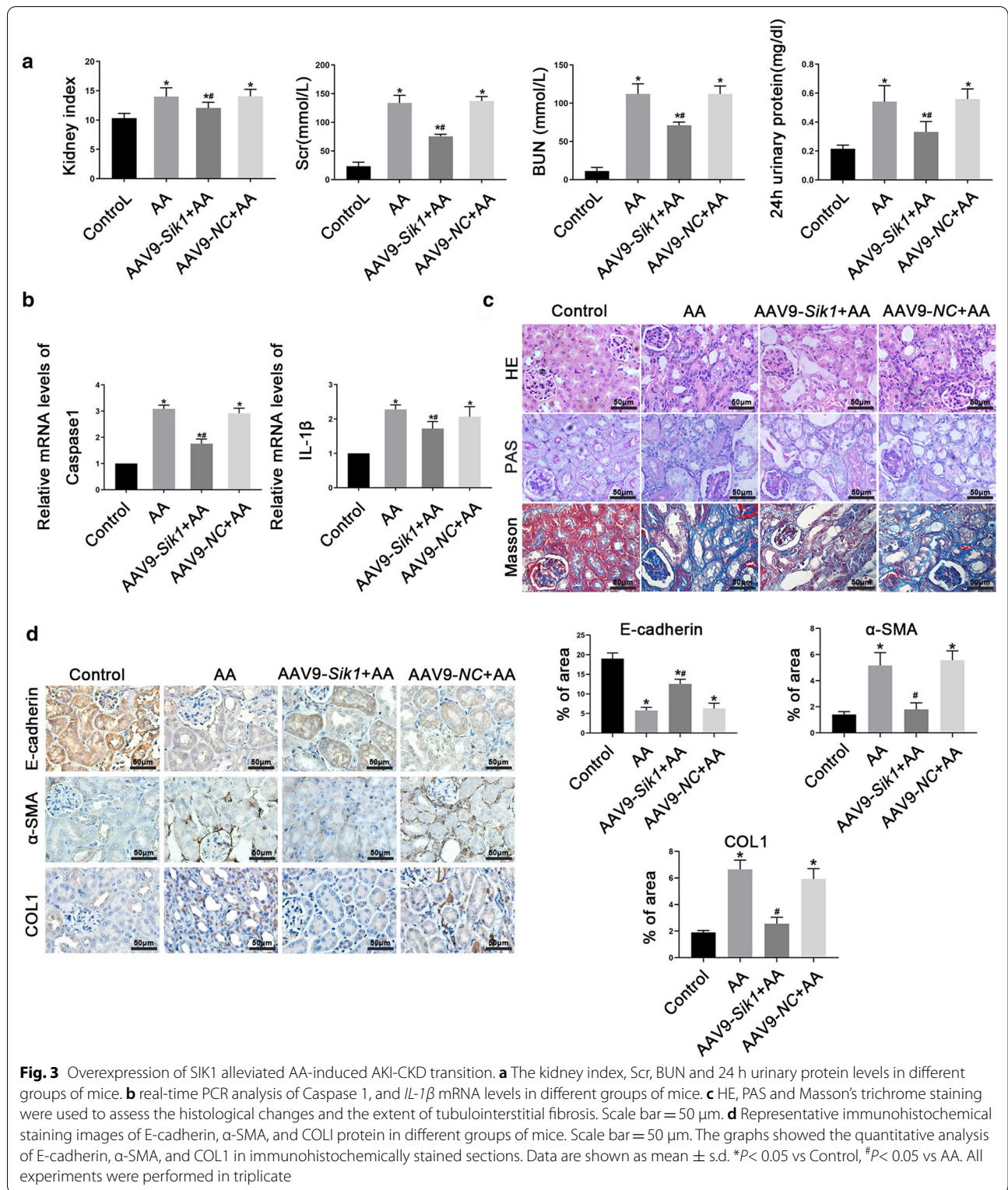
WNT/ β -catenin signaling pathway is involved in AA-induced HK2 cells injury

To explore whether WNT/ β -catenin pathway played a role in AA-induced HK2 cells injury, we tested the expression levels of WNT1, nuclear β -catenin, and p- β -catenin (Y654) after AA treatment. Results of Western blot showed that WNT1, nuclear β -catenin and p- β -catenin (Y654) increased significantly after AA stimulation (Additional file 6a). Besides, immunofluorescence staining revealed the nuclear translocation of β -catenin (Additional file 6b), which suggesting that AA stimulation can activate WNT/ β -catenin signaling pathway. Considering β -catenin is the central component of WNT/ β -catenin pathway, we wonder whether regulation of β -catenin regulates AA-induced HK2 cells injury. Thus, we stably knocked down β -catenin by shRNA lentivirus in HK2 cells (Additional file 6c). And we observed that β -catenin knockdown impaired the AA-induced Caspase1, IL-1 β , Vimentin, PAI-1, and MMP9 expression and promoted E-cadherin expression (Fig. 6a, b). Moreover, β -catenin shRNA cells stimulated with AA exhibited significantly decreased migration compared with the β -catenin control cells stimulated with AA alone (Fig. 6c). Taken together, these findings suggested that WNT/ β -catenin pathway was involved in AA-induced HK2 cells injury.

WNT/ β -catenin signaling pathway is required for SIK1 mediated HK2 cells injury induced by AA

To study whether SIK1 regulated AA-induced HK2 cells injury through WNT/ β -catenin signaling pathway, β -catenin was further decreased in SIK1 knockdown HK2 cells. Compared with SIK1 knockdown cells, further knockdown of β -catenin decreased the mRNA levels





of Caspase1, COL1 and Vimentin, while increased the mRNA levels of E-cadherin (Fig. 7a). The results of Western blot were consistent with real-time PCR, showing

silencing of β-catenin and SIK1 reversed the downregulation of E-cadherin, upregulation of Caspase1/p20/p10 and Vimentin induced by SIK1 knockdown (Fig. 7b).

(See figure on next page.)

Fig. 4 SIK1 was down-regulated in AA-treated HK2 cells and overexpression of SIK1 improved AA-induced HK2 cells injury. **a** ELISA detection of IL-1 β and TNF- α levels in the supernatant of HK2 cells treated with 10 μ mol/L AA for 0 h, 24 h, 48 h and 72 h. **b** Western blot analysis of Caspase 1/p20/p10, E-cadherin, ZO-1, Vimentin, and α -SMA protein levels in HK2 cells treated with 10 μ mol/L AA for 0 h, 24 h, 48 h and 72 h, with the greatest effect after 72 h of treatment. β -actin was used as a control. **c** real-time PCR analysis of early fibrosis indicators (*COL1*, *PAI-1*, and *MMP9*) mRNA levels in HK2 cells treated with 10 μ mol/L AA for 72 h. **d** Western blot analysis of p-SIK1 (Thr182) and SIK1 levels in HK2 cells treated with 10 μ mol/L AA for 0 h, 24 h, 48 h and 72 h. **e** Western blot analysis of Caspase1/p20/p10, E-cadherin, Vimentin, Fsp1, and COL1 in HK2 cells that are treated with SIK1 vector (SIK1 lentiviral overexpression vector) in the presence of 10 μ mol/L AA or treated with 10 μ mol/L AA alone for 72 h. **f** Representative immunofluorescence images of E-cadherin and Vimentin in HK2 cells. Scale bar = 50 μ m. **g** Representative migration results of HK2 cells. Scale bar = 50 μ m. Data are shown as mean \pm s.d. * P < 0.05 vs Control, # P < 0.05 vs AA. All experiments were performed in triplicate

Collectively, these results indicated that inhibition of β -catenin reversed inflammatory response, EMT, and fibrosis progression mediated by SIK1 knockdown, which strongly revealing that WNT/ β -catenin pathway was required for SIK1 mediated HK2 cells injury induced by AA.

The Role of Twist1 in AA-induced HK2 cells injury

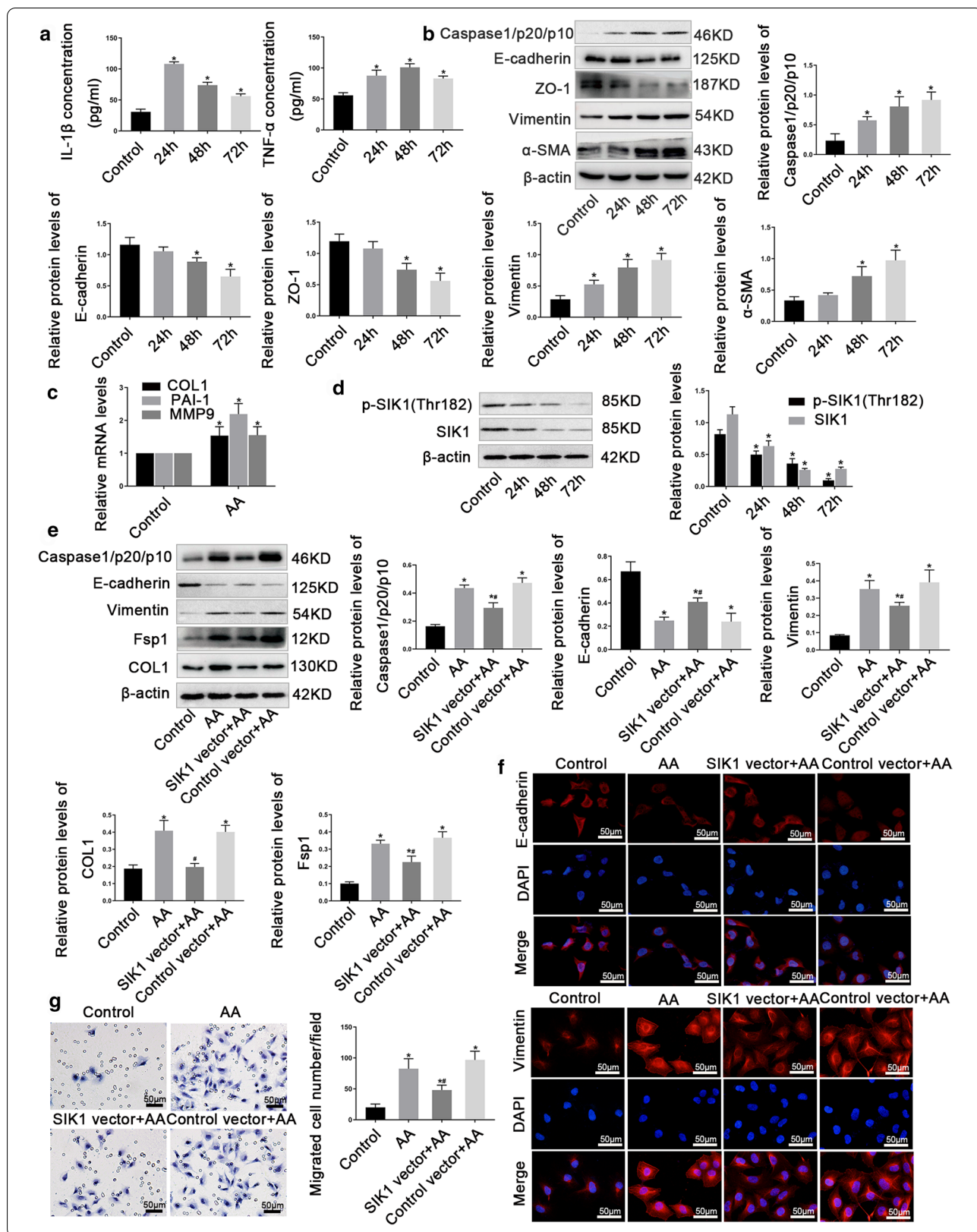
Acting as EMT-TFs, Twist1 can promote EMT and kidney fibrosis. In this study, we found AA promoted the protein and mRNA expression of Snail and Twist1 while knockdown β -catenin inhibited the expression of Snail and Twist1 induced by AA (Fig. 8a), indicating Snail and Twist1 located in the downstream of β -catenin and played a role in AA-induced HK2 cells injury. To verify our hypothesis, we knockdown Twist1 by siRNA (Additional file 7) and carried out real-time PCR and Western blot analysis. As expected, when compared with control cells stimulated with AA alone, the expression of Vimentin, and COL1 was reduced while ZO-1 was increased in Twist1 siRNA cells in the presence of AA, suggesting silence of Twist1 alleviated the occurrence of EMT and the progression of renal fibrosis induced by AA (Fig. 8b and c).

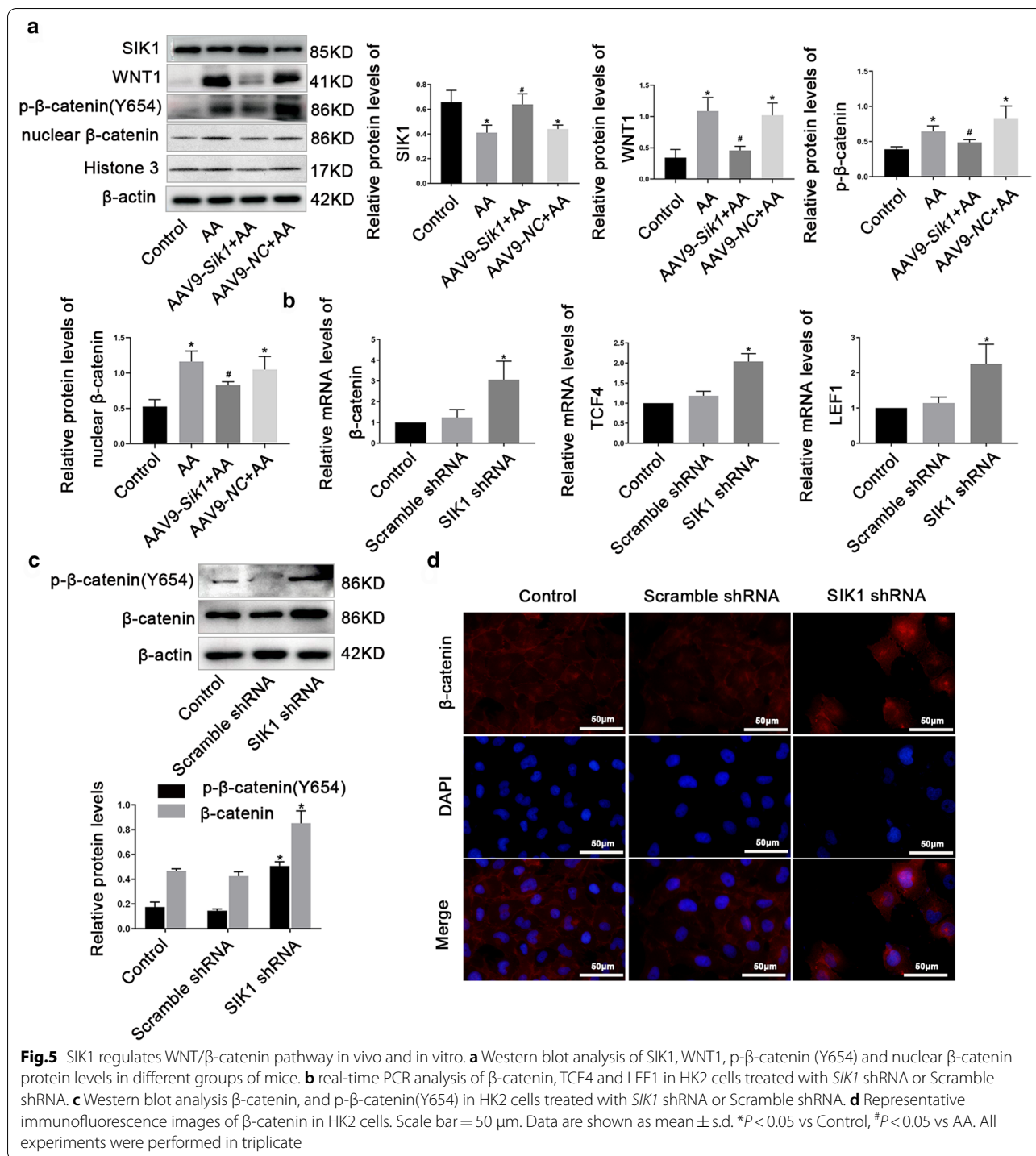
Discussion

AKI is a serious public health problem with high morbidity and mortality. In the past, AKI was considered to be reversible and a temporary decline in renal function. However, recent studies have gradually realized that the recovery of renal function in patients who survive AKI is often incomplete [23–25]. A meta-analysis has reported that patients with AKI had higher risks for developing CKD and ESDR, compared with patients without AKI [26]. Recently, the mechanism of AKI-CKD transition has attracted more and more attention from nephrologists. Many factors such as nephron loss, vascular insufficiency, endothelial injury, cell cycle disruption, interstitial inflammation and fibrosis, and maladaptive repair mechanisms may lead to the evolution of AKI into CKD [27]. The pathophysiological mechanisms are as follows: (1) After AKI, inflammatory cells release inflammatory

factors and chemokines, and continuous inflammation can lead to the loss of renal function [28]; (2) Nephron loss, endothelial injury, vascular malfunction, leading to ischemia and hypoxia of renal tubular microenvironment and fibrosis of tubular interstitial [27]; (3) After AKI, tubular epithelial cell undergo EMT to produce myofibroblasts from the epithelia to heal the injured tissues. If the injury is mild and acute, the healing process is considered as reparative fibrosis; However, under continuous chronic inflammation, the abnormal formation of myofibroblasts can lead to progressive fibrosis, after which ECM accumulation and then the destruction of organ parenchyma will occur [29]; (4) The cell cycle G2/M was arrested in renal tubular epithelial cells after AKI, which can activate pro-fibrotic signaling pathway to induce profibrotic cytokine production [30]. In this study, we used AA to mimic the progression of AKI-CKD transition in vivo and in vitro, and we observed that AA stimulation can induce inflammation, EMT and fibrosis, which suggesting the successful establishment of AKI-CKD transition model.

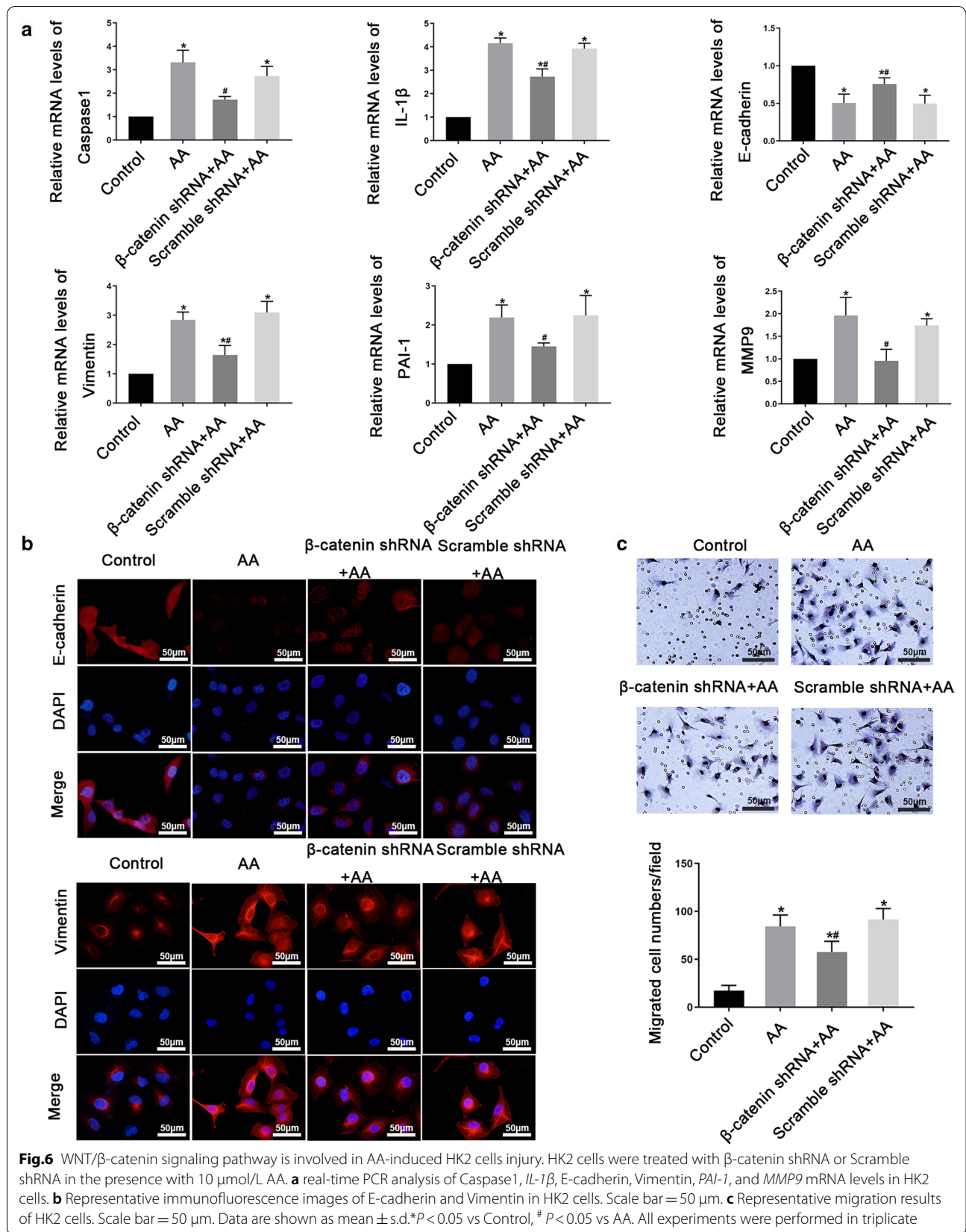
Abundant evidences have demonstrated the role of SIK1 on EMT [8–10] and inflammation [11, 31], which are the hallmarks of AKI-CKD transition. For instance, it was reported that LKB1-SIK1 signaling pathway inhibited EMT by regulating the expression of some key transcription factors, including Snail2, Twist and ZEB1 [32]. More recently, the role of SIK1 in the kidney damage has drawn considerable attention. Ferrandi et al. have reported that nephrin and SIK1 co-localization in glomerular podocytes and there is a positive correlation between nephrin and SIK1 protein expression in rats and human renal specimens [12]. Moreover, SIK1 is involved in high glucose-induced mesangial cell proliferation and extracellular matrix accumulation mediated by the ALK5 signaling pathway [6]. All above indicate that SIK1 has a vital role in the kidney damage. SIK1 has a highly conserved serine (Thr182) in the kinase domain. After activated by the AMPK-activator LKB1 which phosphorylates SIK1 at Thr182, the activated SIK1 auto-phosphorylates its Ser186, and then maintains the sustained activity of SIK1 through sequential phosphorylation at Ser186-Thr182 by

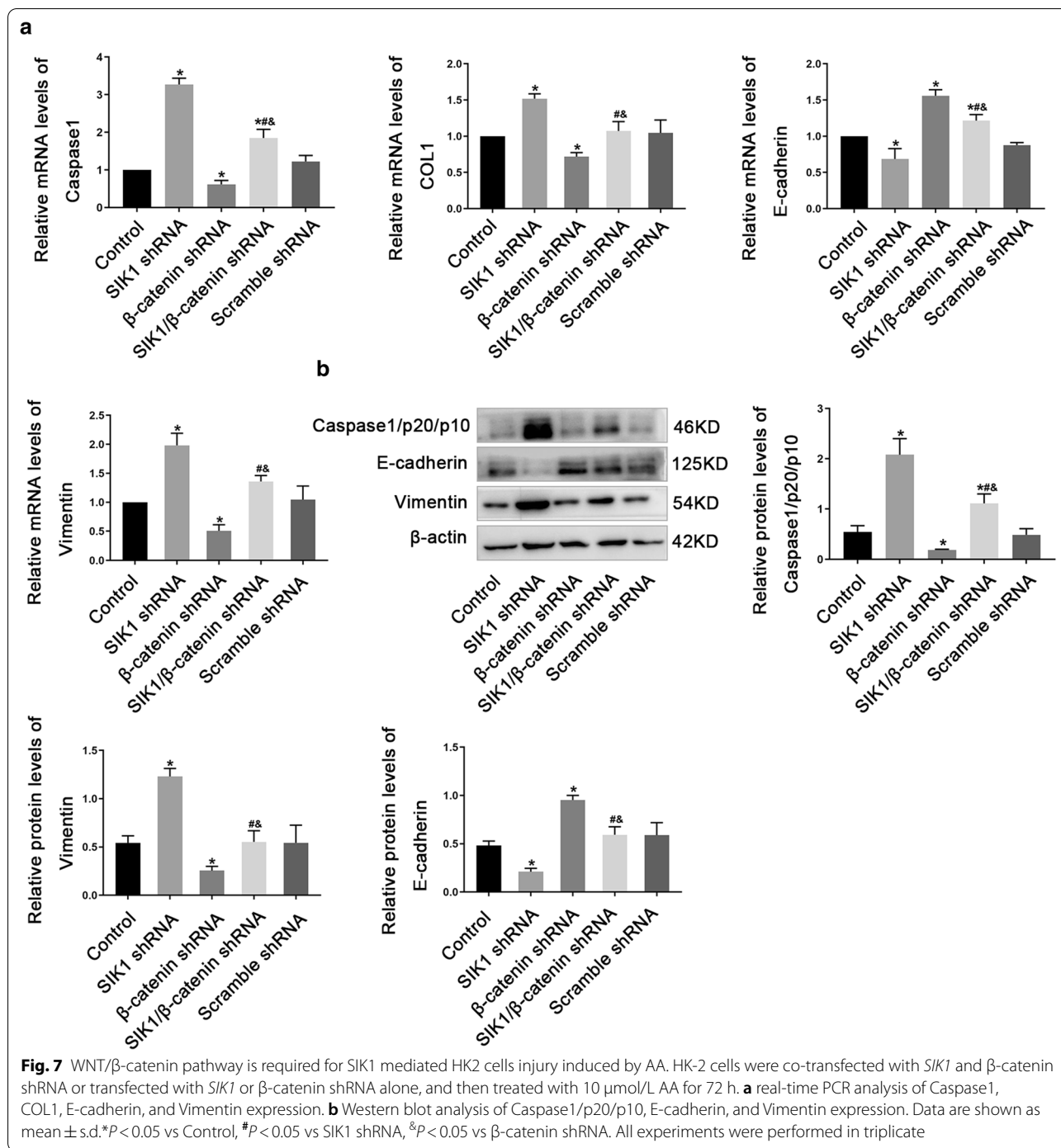




GSK-3β [33]. In this study, we discovered that the expression of SIK1 was downregulated in AKI patients and AKI mice, arousing our interest to further explore whether SIK1 was involved in AKI-CKD transition. By assessing the level of SIK1 in HK2 cells and C57BL/6 mice treated with AA, we observed that SIK1 and p-SIK1(Thr182)

were down-regulated upon AA stimulation. The correlation of the decreased activity of SIK1 with its protein level under AA treatment is consistent with findings in HBZY-1 cells in which the level of Thr182 phosphorylation correlated with the SIK1 protein level under stimulation with high glucose [6]. What's more, in the current





study, we revealed the nuclear redistribution of SIK1 following AA stimulation in HK2 cells, which may result from the reduction in SIK1 kinase activity [6, 34, 35]. Further work is required to characterize the mechanism by which AA localizes SIK1 in the nucleus. Furthermore, we identified that overexpression of SIK1 delayed the progression of inflammation, EMT and fibrosis induced

by AA both in vivo and in vitro. Thus, we concluded that AA induces AKI-CKD transition by inhibiting SIK1 and its phosphorylation level.

Multiple intracellular signal transduction pathways are involved in the expression and activation of EMT and renal fibrosis, including TGF-β signaling pathway, PI3K/AKT pathway, Src pathway, MAPK pathway, and

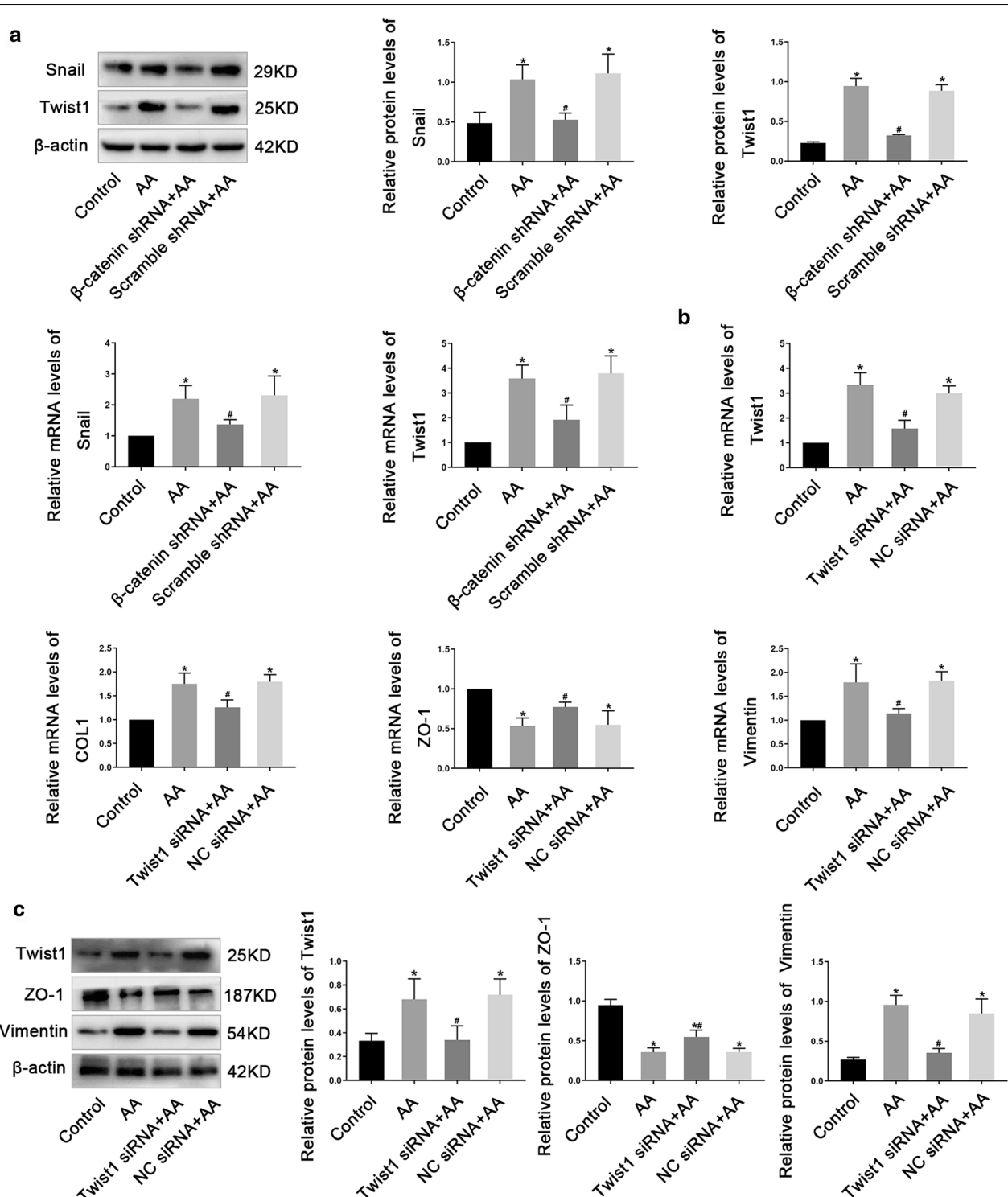


Fig.8 The role of Twist in AA-induced HK2 cells injury. **a** Western blot and real-time PCR analysis of Snail and Twist1 levels in HK2 cells. **b** real-time PCR analysis of Twist1, COL1, ZO-1 and Vimentin levels in HK2 cells treated with *Twist1* siRNA or NC siRNA. **c** Western blot analysis of Twist1, ZO-1 and Vimentin levels in HK2 cells treated with *Twist1* siRNA or NC siRNA. Data are shown as mean \pm s.d. * P < 0.05 vs Control, # P < 0.05 vs AA. All experiments were performed in triplicate

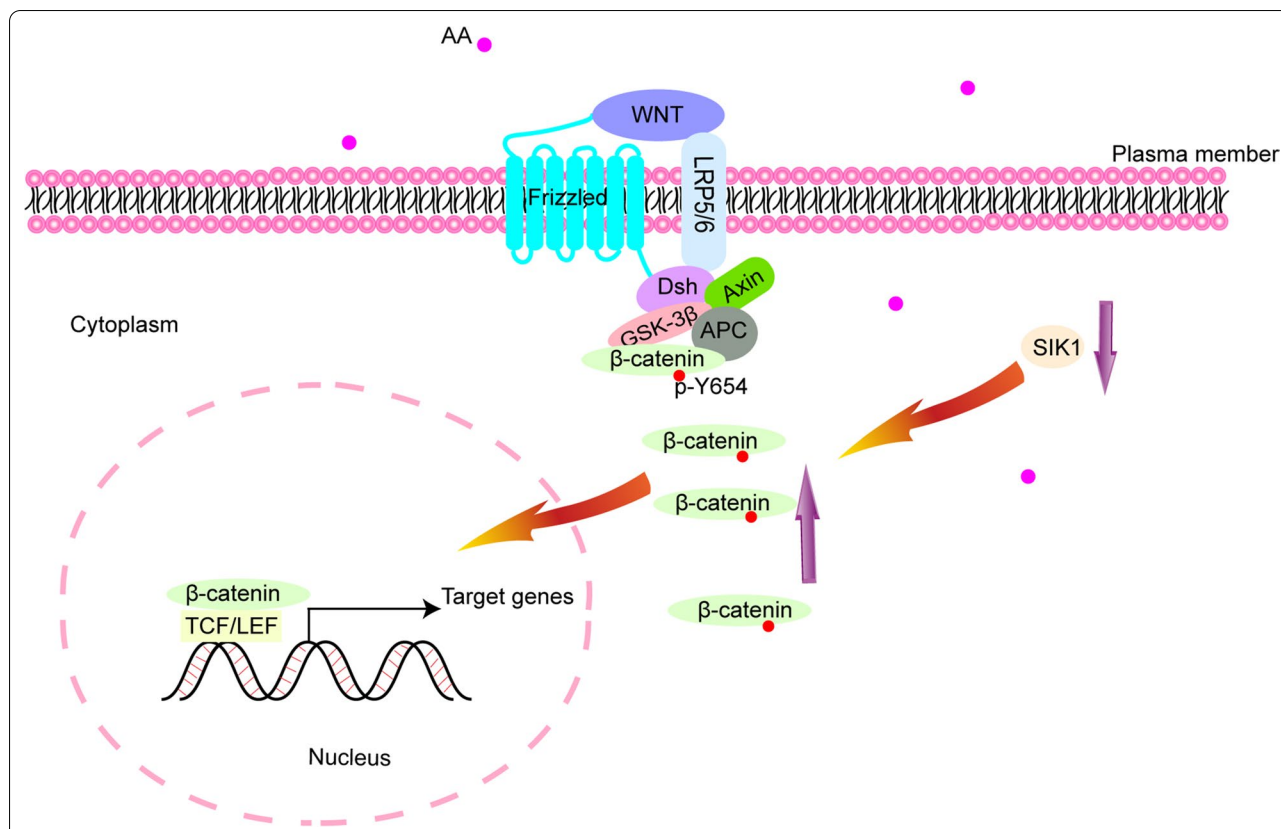


Fig.9 Schematic model of the role of SIK1. AA stimulation down-regulated the expression of SIK1, leading to up-regulation of p-β-catenin (Y654) and nuclear accumulation of β-catenin, thus promoting the transcription of target genes by activating the WNT/β-catenin signaling pathway

WNT signaling pathway [36–41]. Among these, WNT/β-catenin signaling pathway, the most classic WNT pathway, was widely studied. Abundant data have suggested that WNT/β-catenin signaling plays a vital role in EMT [42, 43], inflammation [44, 45] and renal fibrosis [46–48]. β-catenin, a multifunctional protein, is the core molecular in the WNT signaling pathway. When there is no WNT signal stimulation, β-catenin is mainly connected to the proximal C-terminal domain of E-cadherin in the cell membrane; when stimulated by WNT signal, β-catenin translocates into the nucleus and binds to TCF/LEF transcription factors to stimulate the transcription of WNT target genes [49, 50]. The phosphorylation of β-catenin (Y654) leads to its release from E-cadherin protein and increases TCF-mediated transcriptional activity, balancing its role between cell adhesion and WNT signaling [51]. In addition, the increased phosphorylation level of β-catenin (Y654) can increase cell migration and induce tumor cell invasion [52]. In this study, we found that AA stimulation activated WNT/β-catenin signaling pathway and enhanced transcriptional activity of TCF and LEF. In addition, we observed knockdown of β-catenin alleviated the inflammatory response, EMT and fibrosis induced by

AA, suggesting that WNT/β-catenin signaling pathway is involved in AKI-CKD transition, which was consistent with a previous study [17]. Furthermore, we discovered SIK1 regulated WNT/β-catenin signaling pathway both in vivo and in vitro, further supporting the role of SIK1 in AA-induced AKI-CKD transition.

EMT and renal fibrosis require a powerful transcription mechanism to regulate. The transcription factors that activate EMT and fibrosis are mainly divided into three major groups: Snail transcription factors, ZEB transcription factors and bHLH transcription factors. Snail is a zinc finger protein that acts as a transcriptional repressor by recognizing the E-box in the promoter of the target gene and the increased expression of Snail is involved in EMT [53]. Similar to the effect of Snail, Twist1 down-regulated the expression of epithelial phenotype-related genes and induced the expression of mesenchymal phenotype-related genes [54]. The role of Snail and Twist1 in the process of AA-induced AKI-CKD transition is still not fully understood. In this study, we found AA promoted the protein and mRNA expression of Snail and Twist1 while knockdown β-catenin inhibited the expression of Snail and Twist1 induced by AA. Furthermore, we observed that silenced Twist1 by siRNA alleviated the

occurrence of EMT and the progression of renal fibrosis induced by AA, suggesting *Twist1* plays an important role in AA-induced AKI-CKD transition. Further studies are required to determine whether SIK1 could regulate the expression of *Twist1* during AKI-CKD transition.

Conclusion

In this study, we demonstrated that SIK1 was involved in the AA-induced AKI-CKD transition, and we showed that SIK1 participated in AKI-CKD transition through WNT/ β -catenin signaling pathway (Fig. 9). Upregulation of SIK1, or inhibition of WNT/ β -catenin signaling pathway alleviate the inflammation, EMT, and fibrosis induced by AA, delaying the progression of AKI-CKD transition. These observations will provide a new therapeutic target for the clinical prevention and treatment of renal fibrosis after AKI.

Supplementary Information

The online version contains supplementary material available at <https://doi.org/10.1186/s12967-021-02717-5>.

Additional file 1. a Schematic diagram of GV467 carrier information. **b** The ability of AAV9 virus vector to transduce 293 T cells. The high-content imaging system showed that the positive rate of EGFP green fluorescence protein in the AAV9-*Sik1* transfection group. Magnification 200 \times . **c** The ability of AAV9 virus vector to transduce kidney of C57BL/6 mice by tail vein injection. Scale bar = 200 μ m.

Additional file 2. HK2 cells were treated with different concentrations of AA (10, 20, 40, and 60 μ mol/L) for 72 h, and CCK8 were performed to detect the viability of HK2 cells. Data are shown as mean \pm s.d. * P < 0.05 vs Control. All experiments were performed in triplicate.

Additional file 3. Representative immunofluorescence images of SIK1 in HK2 cells treated with 10 μ mol/L AA for 0 h, 24 h, 48 h and 72 h. Scale bar = 50 μ m.

Additional file 4. The overexpression efficiency of SIK1. HK2 cells were treated with SIK1 lentiviral overexpression vector (SIK1 vector) or Control vector, the overexpression efficiency was examined by real-time PCR (a) and Western blot (b). Data are shown as mean \pm s.d. * P < 0.05 vs Control. The experiment was performed in triplicate.

Additional file 5. The knock-down efficiency of SIK1. HK2 cells were treated with *SIK1* lentiviral shRNA (*SIK1* shRNA) or Scramble shRNA, the knock-down efficiency was examined by Western blot. (a) and real-time PCR (b). Data are shown as mean \pm s.d. * P < 0.05 vs Control. * P < 0.05 vs AA. The experiment was performed in triplicate.

Additional file 6. AA stimulation can activate WNT/ β -catenin signaling pathway in HK2 cells. **a** Western blot analysis of WNT1, nuclear β -catenin and p- β -catenin (Y654) levels in HK2 cells. **b** Representative immunofluorescence images of β -catenin in HK2 cells. Scale bar = 50 μ m. **c** HK2 cells were treated with β -catenin lentiviral shRNA (β -catenin shRNA) or Scramble shRNA, the knock-down efficiency was examined by real-time PCR and Western blot. Data are shown as mean \pm s.d. * P < 0.05 vs Control, * P < 0.05 vs AA. The experiment was performed in triplicate.

Additional file 7. The knock-down efficiency of *Twist1*. HK2 cells were treated with *Twist1* siRNA or NC siRNA, the knockdown efficiency was confirmed by real-time PCR (a) and Western blot (b). Data are shown as mean \pm s.d. * P < 0.05 vs Control. The experiment was performed in triplicate.

Abbreviations

AKI: Acute kidney injury; CKD: Chronic kidney disease; SIK1: Salt inducible kinase 1; AA: Aristolochic acid; GFR: Glomerular filtration rate; EMT: Epithelial-mesenchymal transition; AMPKs: AMP-activated protein kinases; ECM: Extracellular matrix; Scr: Serum creatinine; BUN: Blood urea nitrogen; HK2: Human proximal tubular epithelial cells; FBS: Fetal bovine serum; NSCLC: Non-small cell lung cancer.

Acknowledgements

Not applicable.

Authors' contributions

JQ and JH developed the concept and designed the research; JQ, QY, and JH performed the experiments; BL, YL and QM analysed the data; YL, CW and QW interpreted the results of the experiments; JH and JQ drafted the paper; ZL edited and revised the paper. All authors read and approved the final manuscript.

Funding

This work was funded by National Natural Science Foundation of China (Grant: 81873615, 81770723, 81370834, 81400732), The Science and Technology Innovation Program of Clinical Medicine from the Jinan Science and Technology Bureau (NO: 201805054, 201805001), Academic promotion programme of Shandong First Medical University (NO:2019QL022) and the Taishan Scholars Program of Shandong Province (NO: tsqn201812138, ts201712090).

Availability of data and materials

All data generated or analyzed during this study are included either in this article or in the Additional files.

Ethics approval and consent to participate

The human study was approved by the Clinical Research Ethics Committee of Shandong Provincial Hospital Affiliated to Shandong University (No: 2020–901), and the informed consent was signed by all participants in accordance with the Declaration of Helsinki. All animal experiments were approved by the Animal Care and Use Committee of Shandong University (No: 2019–001).

Consent for publication

All authors have read the manuscript and approved its submission to the Journal of Translational Medicine.

Competing interests

The authors declare that they have no competing interests.

Author details

¹ Department of Nephrology, Shandong Provincial Hospital, Cheeloo College of Medicine, Shandong University, Jinan 250021, Shandong, China. ² Department of Nephrology, Shandong Provincial Hospital Affiliated to Shandong First Medical University, Jinan 250021, Shandong, China. ³ Department of Pathology, School of Medicine, Shandong University, Jinan 250021, Shandong, China.

Received: 6 December 2020 Accepted: 23 January 2021

Published online: 15 February 2021

References

- Maciel AT, Delphino Salles L, Vitorio D. Imed Research Group of I Simple blood and urinary parameters measured at ICU admission may sign for AKI development in the early postoperative period: a retrospective, exploratory study. *Ren Fail.* 2016;38(10):1607–15.
- Venkatachalam MA, Weinberg JM, Kriz W, Bidani AK. Failed tubule recovery, AKI-CKD transition, and kidney disease progression. *J Am Soc Nephrol.* 2015;26(8):1765–76.
- Jones J, Holmen J, De Graauw J, Jovanovich A, Thornton S, Chonchol M. Association of complete recovery from acute kidney injury with incident CKD stage 3 and all-cause mortality. *Am J Kidney Dis.* 2012;60(3):402–8.
- Chawla LS, Kimmel PL. Acute kidney injury and chronic kidney disease: an integrated clinical syndrome. *Kidney Int.* 2012;82(5):516–24.

5. Song Y, Tao Q, Yu L, Li L, Bai T, Song X, Hu H, Li Y, Tan X. Activation of autophagy contributes to the renoprotective effect of postconditioning on acute kidney injury and renal fibrosis. *Biochem Biophys Res Commun*. 2018;504(4):641–6.
6. Yu J, Hu X, Yang Z, Takemori H, Li Y, Zheng H, Hong S, Liao Q, Wen X. Salt-inducible kinase 1 is involved in high glucose-induced mesangial cell proliferation mediated by the ALK5 signaling pathway. *Int J Mol Med*. 2013;32(1):151–7.
7. Taub M. Salt inducible kinase signaling networks: implications for acute kidney injury and therapeutic potential. *Int J Mol Sci*. 2019;20(13):3219.
8. Qu C, He D, Lu X, Dong L, Zhu Y, Zhao Q, Jiang X, Chang P, Jiang X, Wang L, et al. Salt-inducible Kinase (SIK1) regulates HCC progression and WNT/ β -catenin activation. *J Hepatol*. 2016;64(5):1076–89.
9. Gradek F, Lopez-Charcas O, Chadet S, Poisson L, Ouldamer L, Goupille C, Jourdan ML, Chevalier S, Moussata D, Besson P, et al. Sodium Channel Nav1.5 controls epithelial-to-mesenchymal transition and invasiveness in breast cancer cells through its regulation by the salt-inducible kinase-1. *Sci Rep*. 2019;9(1):18652.
10. Yao YH, Cui Y, Qiu XN, Zhang LZ, Zhang W, Li H, Yu JM. Attenuated LKB1-SIK1 signaling promotes epithelial-mesenchymal transition and radioreistance of non-small cell lung cancer cells. *Chin J Cancer*. 2016;35:50.
11. Yong Kim S, Jeong S, Chah KH, Jung E, Baek KH, Kim ST, Shim JH, Chun E, Lee KY. Salt-inducible kinases 1 and 3 negatively regulate Toll-like receptor 4-mediated signal. *Mol Endocrinol*. 2013;27(11):1958–68.
12. Ferrandi M, Molinari I, Matafora V, Zerbini G, Trevisani F, Rastaldi MP, Simonini M, Giardino L, Ferrari P, Manunta P. SIK1 localizes with nephrin in glomerular podocytes and its polymorphism predicts kidney injury. *Hum Mol Genet*. 2014;23(16):4371–82.
13. Kowanetz M, Lonn P, Vanlandewijck M, Kowanetz K, Heldin CH, Moustakas A. TGF β induces SIK to negatively regulate type I receptor kinase signaling. *J Cell Biol*. 2008;182(4):655–62.
14. Klaus A, Birchmeier W. Wnt signalling and its impact on development and cancer. *Nat Rev Cancer*. 2008;8(5):387–98.
15. Saito S, Tampe B, Muller GA, Zeisberg M. Primary cilia modulate balance of canonical and non-canonical Wnt signaling responses in the injured kidney. *Fibrogenesis Tissue Repair*. 2015;8:6.
16. Kawakami T, Ren S, Duffield JS. Wnt signalling in kidney diseases: dual roles in renal injury and repair. *J Pathol*. 2013;229(2):221–31.
17. Ogbadu J, Singh G, Aggarwal D. Factors affecting the transition of acute kidney injury to chronic kidney disease: Potential mechanisms and future perspectives. *Eur J Pharmacol*. 2019;865:172711.
18. Ning X, Zhang K, Wu Q, Liu M, Sun S. Emerging role of Twist1 in fibrotic diseases. *J Cell Mol Med*. 2018;22(3):1383–91.
19. Grande MT, Sanchez-Laorden B, Lopez-Blau C, De Frutos CA, Boutet A, Arevalo M, Rowe RG, Weiss SJ, Lopez-Novoa JM, Nieto MA. Snail1-induced partial epithelial-to-mesenchymal transition drives renal fibrosis in mice and can be targeted to reverse established disease. *Nat Med*. 2015;21(9):989–97.
20. Kida Y, Asahina K, Teraoka H, Gitelman I, Sato T. Twist relates to tubular epithelial-mesenchymal transition and interstitial fibrogenesis in the obstructed kidney. *J Histochem Cytochem*. 2007;55(7):661–73.
21. Lovisa S, LeBlau VS, Tampe B, Sugimoto H, Vadnagara K, Carstens JL, Wu CC, Hagos Y, Burckhardt BC, Pentcheva-Hoang T, et al. Epithelial-to-mesenchymal transition induces cell cycle arrest and parenchymal damage in renal fibrosis. *Nat Med*. 2015;21(9):998–1009.
22. Dai XY, Huang XR, Zhou L, Zhang L, Fu P, Manthey C, Nikolic-Paterson DJ, Lan HY. Targeting c-fms kinase attenuates chronic aristolochic acid nephropathy in mice. *Oncotarget*. 2016;7(10):10841–56.
23. Chen Y, Lin L, Tao X, Song Y, Cui J, Wan J. The role of podocyte damage in the etiology of ischemia-reperfusion acute kidney injury and post-injury fibrosis. *BMC Nephrol*. 2019;20(1):106.
24. Sawhney S, Marks A, Fluck N, Levin A, McLernon D, Prescott G, Black C. Post-discharge kidney function is associated with subsequent ten-year renal progression risk among survivors of acute kidney injury. *Kidney Int*. 2017;92(2):440–52.
25. Hingorani S, Molitoris BA, Himmelfarb J. Ironing out the pathogenesis of acute kidney injury. *Am J Kidney Dis*. 2009;53(4):569–71.
26. Coca SG, Singanamala S, Parikh CR. Chronic kidney disease after acute kidney injury: a systematic review and meta-analysis. *Kidney Int*. 2012;81(5):442–8.
27. Chaturvedi S, Ng KH, Mammen C. The path to chronic kidney disease following acute kidney injury: a neonatal perspective. *Pediatr Nephrol*. 2017;32(2):227–41.
28. Zuk A, Bonventre JV. Acute kidney injury. *Annu Rev Med*. 2016;67:293–307.
29. Tennakoon AH, Izawa T, Kuwamura M, Yamate J. Pathogenesis of type 2 epithelial to mesenchymal transition (EMT) in renal and hepatic fibrosis. *J Clin Med*. 2015;5(1):4.
30. Liu BC, Tang TT, Lv LL, Lan HY. Renal tubule injury: a driving force toward chronic kidney disease. *Kidney Int*. 2018;93(3):568–79.
31. Zhang Y, Gao W, Yang K, Tao H, Yang H. Salt-Inducible Kinase 1 (SIK1) is induced by alcohol and suppresses microglia inflammation via NF- κ B Signaling. *Cell Physiol Biochem*. 2018;47(4):1411–21.
32. Eneling K, Brion L, Pinto V, Pinho MJ, Sznajder JI, Mochizuki N, Emoto K, Soares-da-Silva P, Bertorello AM. Salt-inducible kinase 1 regulates E-cadherin expression and intercellular junction stability. *FASEB J*. 2012;26(8):3230–9.
33. Takemori H, Katoh Hashimoto Y, Nakae J, Olson EN, Okamoto M. Inactivation of HDAC5 by SIK1 in AICAR-treated C2C12 myoblasts. *Endocr J*. 2009;56(1):121–30.
34. Katoh Y, Takemori H, Lin XZ, Tamura M, Muraoka M, Satoh T, Tsuchiya Y, Min L, Doi J, Miyauchi A, et al. Silencing the constitutive active transcription factor CREB by the LKB1-SIK signaling cascade. *FEBS J*. 2006;273(12):2730–48.
35. Al-Hakim AK, Goransson O, Deak M, Toth R, Campbell DG, Morrice NA, Prescott AR, Alessi DR. 14-3-3 cooperates with LKB1 to regulate the activity and localization of QSK and SIK. *J Cell Sci*. 2005;118(Pt 23):5661–73.
36. Kim MK, Maeng YI, Sung WJ, Oh HK, Park JB, Yoon GS, Cho CH, Park KK. The differential expression of TGF- β 1, ILK and wnt signaling inducing epithelial to mesenchymal transition in human renal fibrogenesis: an immunohistochemical study. *Int J Clin Exp Pathol*. 2013;6(9):1747–58.
37. Li R, Guo Y, Zhang Y, Zhang X, Zhu L, Yan T. Salidroside ameliorates renal interstitial fibrosis by inhibiting the TLR4/NF- κ B and MAPK signaling pathways. *Int J Mol Sci*. 2019;20(5):1103.
38. Zhang X, Lu H, Xie S, Wu C, Guo Y, Xiao Y, Zheng S, Zhu H, Zhang Y, Bai Y. Resveratrol suppresses the myofibroblastic phenotype and fibrosis formation in kidneys via proliferation-related signalling pathways. *Br J Pharmacol*. 2019;176(24):4745–59.
39. Wang B, Koh P, Winbanks C, Coughlan MT, McClelland A, Watson A, Jandeleit-Dahm K, Burns WC, Thomas MC, Cooper ME, et al. miR-200a Prevents renal fibrogenesis through repression of TGF- β 2 expression. *Diabetes*. 2011;60(1):280–7.
40. Sutariya B, Jhonsa D, Saraf MN. TGF- β : the connecting link between nephropathy and fibrosis. *Immunopharmacol Immunotoxicol*. 2016;38(1):39–49.
41. Park JS, Choi HI, Kim DH, Kim CS, Bae EH, Ma SK, Kim SW. RON receptor tyrosine kinase regulates epithelial mesenchymal transition and the expression of pro-fibrotic markers via Src/Smad signaling in HK-2 and NRK49F cells. *Int J Mol Sci*. 2019;20(21):5489.
42. Ying Q, Wu G. Molecular mechanisms involved in podocyte EMT and concomitant diabetic kidney diseases: an update. *Ren Fail*. 2017;39(1):474–83.
43. Fu D, Senouthei S, Wang J, You Y. FKN Facilitates HK-2 Cell EMT and tubulointerstitial lesions via the Wnt/ β -Catenin pathway in a murine model of lupus nephritis. *Front Immunol*. 2019;10:784.
44. Wong DWL, Yiu WH, Chan KW, Li Y, Li B, Lok SWY, Taketo MM, Igarashi P, Chan LYY, Leung JCK, et al. Activated renal tubular Wnt/ β -catenin signaling triggers renal inflammation during overload proteinuria. *Kidney Int*. 2018;93(6):1367–83.
45. Vallée A, Lecarpentier Y. Crosstalk between peroxisome proliferator-activated receptor gamma and the canonical WNT/ β -catenin pathway in chronic inflammation and oxidative stress during carcinogenesis. *Front Immunol*. 2018;9:745.
46. Hao S, He W, Li Y, Ding H, Hou Y, Nie J, Hou FF, Kahn M, Liu Y. Targeted inhibition of β -catenin/CBP signaling ameliorates renal interstitial fibrosis. *J Am Soc Nephrol*. 2011;22(9):1642–53.
47. Madan B, Patel MB, Zhang J, Bunte RM, Rudemiller NP, Griffiths R, Virshup DM, Crowley SD. Experimental inhibition of porcupine-mediated Wnt O-acetylation attenuates kidney fibrosis. *Kidney Int*. 2016;89(5):1062–74.
48. Surendran K, Schiavi S, Hruska KA. Wnt-dependent β -catenin signaling is activated after unilateral ureteral obstruction, and recombinant

- secreted frizzled-related protein 4 alters the progression of renal fibrosis. *J Am Soc Nephrol.* 2005;16(8):2373–84.
49. Clevers H, Nusse R. Wnt/beta-catenin signaling and disease. *Cell.* 2012;149(6):1192–205.
50. Tafrihi M, Nakhaei SR. E-Cadherin/beta-Catenin Complex: A target for anticancer and antimetastasis plants/plant-derived compounds. *Nutr Cancer.* 2017;69(5):702–22.
51. Lilien J, Balsamo J. The regulation of cadherin-mediated adhesion by tyrosine phosphorylation/dephosphorylation of beta-catenin. *Curr Opin Cell Biol.* 2005;17(5):459–65.
52. van Veelen W, Le NH, Helvensteijn W, Blonden L, Theeuwes M, Bakker ER, Franken PF, van Gurp L, Meijlink F, van der Valk MA, et al. beta-catenin tyrosine 654 phosphorylation increases Wnt signalling and intestinal tumorigenesis. *Gut.* 2011;60(9):1204–12.
53. Yoshino J, Monkawa T, Tsuji M, Inukai M, Itoh H, Hayashi M. Snail1 is involved in the renal epithelial-mesenchymal transition. *Biochem Biophys Res Commun.* 2007;362(1):63–8.
54. Yang J, Mani SA, Donaher JL, Ramaswamy S, Itzykson RA, Come C, Savagner P, Gitelman I, Richardson A, Weinberg RA. Twist, a master regulator of morphogenesis, plays an essential role in tumor metastasis. *Cell.* 2004;117(7):927–39.

Publisher's Note

Springer Nature remains neutral with regard to jurisdictional claims in published maps and institutional affiliations.

Ready to submit your research? Choose BMC and benefit from:

- fast, convenient online submission
- thorough peer review by experienced researchers in your field
- rapid publication on acceptance
- support for research data, including large and complex data types
- gold Open Access which fosters wider collaboration and increased citations
- maximum visibility for your research: over 100M website views per year

At BMC, research is always in progress.

Learn more biomedcentral.com/submissions

